

World Journal of *Gastroenterology*

World J Gastroenterol 2021 July 14; 27(26): 3951-4251



FRONTIER

- 3951** Liver dysfunction and SARS-CoV-2 infection
Gracia-Ramos AE, Jaquez-Quintana JO, Contreras-Omaña R, Auron M

OPINION REVIEW

- 3971** Chronic hepatitis B infection with concomitant hepatic steatosis: Current evidence and opinion
Shi YW, Yang RX, Fan JG

REVIEW

- 3984** Acute kidney injury and hepatorenal syndrome in cirrhosis
Gupta K, Bhurwal A, Law C, Ventre S, Minacapelli CD, Kabaria S, Li Y, Tait C, Catalano C, Rustgi VK
- 4004** Progress and challenges in the comprehensive management of chronic viral hepatitis: Key ways to achieve the elimination
Higuera-de la Tijera F, Servín-Caamaño A, Servín-Abad L
- 4018** Viral hepatitis update: Progress and perspectives
Pisano MB, Giadans CG, Flichman DM, Ré VE, Preciado MV, Valva P
- 4045** Biomarkers in the diagnosis of pancreatic cancer: Are we closer to finding the golden ticket?
O'Neill RS, Stoita A
- 4088** Non-occlusive mesenteric ischemia: Diagnostic challenges and perspectives in the era of artificial intelligence
Bourcier S, Klug J, Nguyen LS
- 4104** Hepatocellular carcinoma in patients with renal dysfunction: Pathophysiology, prognosis, and treatment challenges
Yeh H, Chiang CC, Yen TH

MINIREVIEWS

- 4143** Abdominal and gastrointestinal manifestations in COVID-19 patients: Is imaging useful?
Boraschi P, Giugliano L, Mercogliano G, Donati F, Romano S, Neri E
- 4160** Inflammatory effect on the gastrointestinal system associated with COVID-19
Delgado-Gonzalez P, Gonzalez-Villarreal CA, Roacho-Perez JA, Quiroz-Reyes AG, Islas JF, Delgado-Gallegos JL, Arellanos-Soto D, Galan-Huerta KA, Garza-Treviño EN
- 4172** Adult pancreatoblastoma: Current concepts in pathology
Omiyale AO

- 4182 Prevention of vertical transmission of hepatitis B virus infection

Veronese P, Dodi I, Esposito S, Indolfi G

- 4194 Endoscopic ultrasound fine needle aspiration *vs* fine needle biopsy for pancreatic masses, subepithelial lesions, and lymph nodes

Levine I, Trindade AJ

ORIGINAL ARTICLE

Basic Study

- 4208 Metal-organic framework IRMOFs coated with a temperature-sensitive gel delivering norcantharidin to treat liver cancer

Li XY, Guan QX, Shang YZ, Wang YH, Lv SW, Yang ZX, Wang R, Feng YF, Li WN, Li YJ

- 4221 Ubiquitin-specific protease 15 contributes to gastric cancer progression by regulating the Wnt/ β -catenin signaling pathway

Zhong M, Zhou L, Fang Z, Yao YY, Zou JP, Xiong JP, Xiang XJ, Deng J

Retrospective Study

- 4236 Feasibility of totally laparoscopic gastrectomy without prophylactic drains in gastric cancer patients

Liu H, Jin P, Quan X, Xie YB, Ma FH, Ma S, Li Y, Kang WZ, Tian YT

CORRECTION

- 4246 Correction to "Downregulation of FoxM1 inhibits the viability and invasion of gallbladder carcinoma cells, partially dependent on the induction of cellular senescence"

Tao J, Xu XS, Song YZ, Liu C

LETTER TO THE EDITOR

- 4248 Impact of COVID-19 on the clinical status of patients with Wilson disease

Zhuang YP, Zhong HJ

ABOUT COVER

Editorial Board Member of *World Journal of Gastroenterology*, Mortada HF El-Shabrawi, MD, FAASLD, Professor of Pediatrics and Pediatric Hepatology, Faculty of Medicine, Cairo University, 3 Nablous Street, Off Shehab Street, Mohandessen, Giza 12411, Egypt. melshabrawi@medicine.cu.edu.eg

AIMS AND SCOPE

The primary aim of *World Journal of Gastroenterology* (WJG, *World J Gastroenterol*) is to provide scholars and readers from various fields of gastroenterology and hepatology with a platform to publish high-quality basic and clinical research articles and communicate their research findings online. WJG mainly publishes articles reporting research results and findings obtained in the field of gastroenterology and hepatology and covering a wide range of topics including gastroenterology, hepatology, gastrointestinal endoscopy, gastrointestinal surgery, gastrointestinal oncology, and pediatric gastroenterology.

INDEXING/ABSTRACTING

The WJG is now indexed in Current Contents®/Clinical Medicine, Science Citation Index Expanded (also known as SciSearch®), Journal Citation Reports®, Index Medicus, MEDLINE, PubMed, PubMed Central, and Scopus. The 2021 edition of Journal Citation Report® cites the 2020 impact factor (IF) for WJG as 5.742; Journal Citation Indicator: 0.79; IF without journal self cites: 5.590; 5-year IF: 5.044; Ranking: 28 among 92 journals in gastroenterology and hepatology; and Quartile category: Q2. The WJG's CiteScore for 2020 is 6.9 and Scopus CiteScore rank 2020: Gastroenterology is 19/136.

RESPONSIBLE EDITORS FOR THIS ISSUE

Production Editor: Ji-Hong Lin; Production Department Director: Yun-Jie Ma; Editorial Office Director: Ze-Mao Gong.

NAME OF JOURNAL

World Journal of Gastroenterology

ISSN

ISSN 1007-9327 (print) ISSN 2219-2840 (online)

LAUNCH DATE

October 1, 1995

FREQUENCY

Weekly

EDITORS-IN-CHIEF

Andrzej S Tarnawski, Subrata Ghosh

EDITORIAL BOARD MEMBERS

<http://www.wjgnet.com/1007-9327/editorialboard.htm>

PUBLICATION DATE

July 14, 2021

COPYRIGHT

© 2021 Baishideng Publishing Group Inc

INSTRUCTIONS TO AUTHORS

<https://www.wjgnet.com/bpg/gerinfo/204>

GUIDELINES FOR ETHICS DOCUMENTS

<https://www.wjgnet.com/bpg/GerInfo/287>

GUIDELINES FOR NON-NATIVE SPEAKERS OF ENGLISH

<https://www.wjgnet.com/bpg/gerinfo/240>

PUBLICATION ETHICS

<https://www.wjgnet.com/bpg/GerInfo/288>

PUBLICATION MISCONDUCT

<https://www.wjgnet.com/bpg/gerinfo/208>

ARTICLE PROCESSING CHARGE

<https://www.wjgnet.com/bpg/gerinfo/242>

STEPS FOR SUBMITTING MANUSCRIPTS

<https://www.wjgnet.com/bpg/GerInfo/239>

ONLINE SUBMISSION

<https://www.f6publishing.com>



Basic Study

Metal-organic framework IRMOFs coated with a temperature-sensitive gel delivering norcantharidin to treat liver cancer

Xiu-Yan Li, Qing-Xia Guan, Yu-Zhou Shang, Yan-Hong Wang, Shao-Wa Lv, Zhi-Xin Yang, Rui Wang, Yu-Fei Feng, Wei-Nan Li, Yong-Ji Li

ORCID number: Xiu-Yan Li 0000-0003-1060-8442; Qing-Xia Guan 0000-0002-4282-9154; Yu-Zhou Shang 0000-0001-6003-258X; Yan-Hong Wang 0000-0002-9247-1453; Shao-Wa Lv 0000-0002-1386-6132; Zhi-Xin Yang 0000-0002-4514-795X; Rui Wang 0000-0002-8486-4660; Yu-Fei Feng 0000-0002-9507-6950; Wei-Nan Li 0000-0002-9888-4806; Yong-Ji Li 0000-0003-0746-0360.

Author contributions: Li XY, Guan QX, Shang YZ, Wang YH, Lv SW, Yang ZX, Wang R, Feng YF, Li WN, and Li YJ performed the experiments and acquired and analyzed the data; Li XY, Guan QX, Shang YZ, and Wang YH wrote the manuscript; All authors approved the final version of the article.

Supported by National Natural Science Foundation of China, No. 82074025 and No. 82074271; the Heilongjiang Traditional Chinese Medicine Research Project, No. ZHY18-047; and Scientific Research Project of Heilongjiang Health Committee, No. 2020-293.

Institutional review board statement: This study was approved by Ethics Committee of Heilongjiang University of Chinese Medicine, Harbin, China.

Xiu-Yan Li, Qing-Xia Guan, Yu-Zhou Shang, Yan-Hong Wang, Shao-Wa Lv, Zhi-Xin Yang, Rui Wang, Yu-Fei Feng, Wei-Nan Li, Yong-Ji Li, College of Pharmacy, Heilongjiang University of Chinese Medicine, Harbin 150040, Heilongjiang Province, China

Corresponding author: Yong-Ji Li, PhD, Professor, College of Pharmacy, Heilongjiang University of Chinese Medicine, No. 24 Heping Road, Xiangfang District, Harbin 150040, Heilongjiang Province, China. liyongji2009@163.com

Abstract

BACKGROUND

Norcantharidin (NCTD) is suitable for the treatment of primary liver cancer, especially early and middle primary liver cancer. This compound can reduce tumors and improve immune function. However, the side effects of NCTD have limited its application. There is a marked need to reduce the side effects and increase the efficacy of NCTD.

AIM

To develop a nanomaterial carrier, NCTD-loaded metal-organic framework IRMOF-3 coated with a temperature-sensitive gel (NCTD-IRMOF-3-Gel), aiming to improve the anticancer activity of NCTD and reduce the drug dose.

METHODS

NCTD-IRMOF-3-Gel was obtained by a coordination reaction. The apparent characteristics and *in vitro* release of NCTD-IRMOF-3-Gel were investigated. Cell cytotoxicity assays, flow cytometry, and apoptosis experiments in mouse hepatoma (Hepa1-6) cells were used to determine the anti-liver cancer activity of NCTD-IRMOF-3-Gel in *in vitro* models.

RESULTS

The particle size of NCTD-IRMOF-3-Gel was 50-100 nm, and the particle size distribution was uniform. The release curve showed that NCTD-IRMOF-3-Gel had an obvious sustained-release effect. The cytotoxicity assays showed that the free drug NCTD and NCTD-IRMOF-3-Gel treatments markedly inhibited Hepa1-6 cell proliferation, and the inhibition rate increased with increasing drug concentration. By flow cytometry, NCTD-IRMOF-3-Gel was observed to block the Hepa1-6 cell cycle in the S and G2/M phases, and the thermosensitive gel

Conflict-of-interest statement: The authors report no conflicts of interest in this work.

Data sharing statement: No additional data are available.

Open-Access: This article is an open-access article that was selected by an in-house editor and fully peer-reviewed by external reviewers. It is distributed in accordance with the Creative Commons Attribution NonCommercial (CC BY-NC 4.0) license, which permits others to distribute, remix, adapt, build upon this work non-commercially, and license their derivative works on different terms, provided the original work is properly cited and the use is non-commercial. See: <http://creativecommons.org/licenses/by-nc/4.0/>

Manuscript source: Unsolicited manuscript

Specialty type: Gastroenterology and hepatology

Country/Territory of origin: China

Peer-review report's scientific quality classification

Grade A (Excellent): 0
Grade B (Very good): B, B, B
Grade C (Good): 0
Grade D (Fair): 0
Grade E (Poor): 0

Received: February 25, 2021

Peer-review started: February 25, 2021

First decision: April 18, 2021

Revised: April 27, 2021

Accepted: May 27, 2021

Article in press: May 27, 2021

Published online: July 14, 2021

P-Reviewer: Martinello M, Martins VH, Tabet P

S-Editor: Gong ZM

L-Editor: Filipodia

P-Editor: Liu JH



nanoparticles may inhibit cell proliferation by inducing cell cycle arrest. Apoptosis experiments showed that NCTD-IRMOF-3-Gel induced the apoptosis of Hepa1-6 cells.

CONCLUSION

Our results indicated that the NCTD-IRMOF-3-Gel may be beneficial for liver cancer disease treatment.

Key Words: Norcantharidin; Metal-organic frameworks; IRMOF-3; Temperature-sensitive gel; Drug delivery; Liver cancer

©The Author(s) 2021. Published by Baishideng Publishing Group Inc. All rights reserved.

Core Tip: Norcantharidin (NCTD) is suitable for the treatment of primary liver cancer, especially early and middle primary liver cancer. However, the side effects of NCTD have limited its application. Therefore, we established a liver-targeting therapy in which NCTD is loaded into IRMOF-3 coated with a thermosensitive gel, which can be efficiently delivered to liver cancer cells and slowly released. The results demonstrate that this thermosensitive gel-encapsulated IRMOF-3 has great advantages as an antitumor drug carrier and provides some ideas for passive targeting therapy of tumors.

Citation: Li XY, Guan QX, Shang YZ, Wang YH, Lv SW, Yang ZX, Wang R, Feng YF, Li WN, Li YJ. Metal-organic framework IRMOFs coated with a temperature-sensitive gel delivering norcantharidin to treat liver cancer. *World J Gastroenterol* 2021; 27(26): 4208-4220

URL: <https://www.wjnet.com/1007-9327/full/v27/i26/4208.htm>

DOI: <https://dx.doi.org/10.3748/wjg.v27.i26.4208>

INTRODUCTION

Liver cancer has the characteristics of a high incidence, poor prognosis, and high mortality. The latest World Health Organization data show that the global incidence rate of liver cancer is ranked fifth among malignant tumors, and the incidence rate is ranked third. China is a country with a high incidence of liver cancer and hepatitis B [1, 2]. At present, surgical resection [3, 4], drug chemotherapy [5, 6], nanotechnology [7], and interventional therapy [8] are the main treatment methods for liver or other cancers. Among many chemotherapeutic drugs, norcantharidin (NCTD) has strong antitumor activity and can inhibit a variety of tumors including gastrointestinal cancer [9], malignant lymphoma [10], lung cancer [11], and liver cancer [12].

NCTD was synthesized by removing the 1,2-methyl group from cantharidin, which was extracted from the cantharides of Coleoptera. Compared with cantharidin, NCTD exhibits not only significantly improved anticancer effect but also a great reduction in renal toxicity and strong irritation to the urinary system [13]. The clinical use of NCTD is mainly based on tablets and injections, and this drug has unique advantages in the treatment of cancer. However, the side effects of NCTD have limited its application [14]. First, compared to cantharidin, the toxicity of NCTD is reduced to a large extent but still has a certain degree of urinary system toxicity, and organ toxicity occurs with large doses or long-term use, so there is a strict limit on the maximum dosage of NCTD in the clinic [15]. Second, NCTD is rapidly distributed in various tissues after absorption when administered to mice by gavage. The concentration of NCTD peaks in liver and cancer tissues 15 min after administration. However, this concentration significantly decreases 6 h after administration. Most NCTD is excreted through the kidney within 24 h, with little accumulation in the body. The elimination speed of NCTD from the body is fast, which reduces the compliance of patients with medication [16]. In addition, NCTD is widely distributed in the body after oral administration, and is less distributed in the liver tissue due to its fast elimination speed, which not only reduces its efficacy but also increases the toxicity to other organs [17]. Third, most NCTD injections used in the clinic are sodium salt, with a pH value of approximately 9.0, which makes it highly irritating [18].

In recent years, a large number of studies have been carried out to reduce the side effects and increase the efficacy of NCTD[19-22]. This project aimed to develop a multifunctional metal-organic framework (IRMOF-3) that can play an important role in drug carrying and delivery. Because of the special topological structure of IRMOF-3, drugs can be loaded into the spatial structure to the maximum extent, and it plays great role in controlled release[23-26]. However, when NCTD-IRMOF-3 enters the body, burst release is caused due to endocytosis or gastrointestinal absorption. Therefore, we established a liver-targeting therapy in which NCTD is loaded into IRMOF-3 coated with a thermosensitive gel (NCTD-IRMOF-3-Gel), which can be efficiently delivered to liver cancer cells and slowly released. In this study, NCTD-IRMOF-3-Gel was prepared, and the *in vitro* targeting behavior was explored. It was shown that the combination of IRMOF-3 and the thermosensitive gel could decrease the toxicity and increase the bioavailability of NCTD, representing an effective method for the chemotherapy of liver cancer. This study lays a foundation for the liver-targeting ability of NCTD-IRMOF-3-Gel. The results demonstrate that this thermosensitive gel-encapsulated IRMOF-3 has great advantages as an antitumor drug carrier and provides some ideas for passive targeting therapy of tumors.

MATERIALS AND METHODS

Materials

All of the chemicals used were of analytical grade. N,N-Dimethylformamide (DMF), dichloromethane (CH_2Cl_2) (both Tianjin Fuyu Fine Chemical Co., Ltd., Tianjin, China), zinc acetate dihydrate ($\text{Zn}(\text{OAc})_2 \cdot 2\text{H}_2\text{O}$) (Kaitong Chemical Industry Co. Ltd., Tianjin, China), and 2-amino-terephthalic acid ($\text{NH}_2\text{-BDC}$, $\text{C}_8\text{H}_7\text{NO}_4$) (Henghua Technology Co., Ltd., Jinan, China) were used to prepare nanosized IRMOF-3.

Preparation of NCTD-IRMOF-3-Gel

First, $\text{Zn}(\text{OAc})_2 \cdot 2\text{H}_2\text{O}$ (4 mmol) and $\text{NH}_2\text{-BDC}$ (1 mmol) were completely dissolved in 10 mL and 15 mL DMF, respectively. Then the zinc salt solution was quickly poured into the ligand solution at room temperature (25 °C) to form a milky white precipitate. After magnetic stirring for 1 min and centrifugation for 5 min (12000 r/min), the supernatant was removed and the precipitate was obtained. The deposit was washed three times with DMF (removing unreacted raw materials) and soaked for 3 d with CH_2Cl_2 (removing DMF), with the solvent replaced once per day. Next, the deposit was centrifugally filtered and dried under natural conditions. Then, the samples were activated under vacuum for 12 h at 100 °C, and IRMOF-3 was obtained. For the encapsulation studies, 30 mg NCTD and 10 mg nanoIRMOF-3 were accurately weighed in a 5 mL volumetric flask, and 80% alcohol solution was added. The suspension was stirred for 72 h at room temperature. NCTD-loaded nanoIRMOF-3 (NCTD-IRMOF-3) was then collected by centrifugation and vacuum-dried at room temperature. NCTD-IRMOF-3 (15 mg) was accurately weighed, 3 mL freeze-dried protective agent (4% mannitol and 2% poloxamer) was added, and the mixture was fully dissolved. A small amount of supernatant was collected, frozen in a vial at -40 °C for 24 h, and then frozen in a vacuum freeze dryer for 30 h to obtain the freeze-dried product. NCTD-IRMOF-3 was then dispersed into a thermosensitive gel solution at room temperature to form a dispersion of nanoparticles. When the NCTD-IRMOF-3 nanoparticle dispersion was injected into the body or heated to 37 °C, the NCTD-IRMOF-3-Gel gel could be formed.

Characterization

Physical characterization was performed by powder X-ray diffraction (PXRD) analysis (Phillips Xpert Pro MPD diffractometer with Cu K α radiation $\lambda = 1.5418$ nm at 40 kV and 50 mA). Scanning electron microscopy (SEM) images were obtained using a Quanta 200F (FEI Sirion SEM), confirming the regular shape and nanosize of the particles. Nitrogen adsorption/desorption isotherms and pore size distributions were measured using an MFA-140 system (Beijing Builder Electronic Technology Co., Ltd., Beijing, China). The particle size distribution was measured by a Zetasizer Nano-ZS90 Laser particle size analyzer (Malvern Instruments Co., Ltd., Malvern, United Kingdom).

NCTD release assay

In vitro studies of the release of NCTD from NCTD, NCTD-IRMOF-3, and NCTD-

IRMOF-3-Gel were carried out using dialysis bags (Sigma, St. Louis, MO, United States) soaked in double-distilled water for 12 h. Freeze-dried NCTD, NCTD-IRMOF-3, and NCTD-IRMOF-3-Gel suspensions were added into a dialysis bag, which then was placed in 50 mL phosphate-buffered saline (pH 5.0) to maintain sink conditions and shaken at 100 rpm in a constant-temperature shaker (SHAB; Donglian Electric Technique Co. Ltd., Harbin, China) at 37 °C. Subsequently, 2 mL release medium was withdrawn at regular intervals, and fresh release medium was added to maintain a constant volume. Every trial was repeated three times. The samples were analyzed using high-performance liquid chromatography, and the control experiments were similarly performed using the same proportions to investigate drug release.

In vitro examination

MTT assay for cytotoxicity detection: The mouse hepatoma (Hepa1-6) cell line (Beijing Boyu Kangtai International Biological Technology Co., Ltd., Beijing, China) used in this experiment was maintained in Roswell Park Memorial Institute-1640 medium (HyClone; Thermo Fisher Scientific, Inc., Waltham, MA, United States) supplemented with 10% heat-inactivated fetal calf serum (Sijiqing Tianhang Biological Science and Technology Co., Ltd., Hangzhou, China), 105 U/L penicillin G, and 100 mg/L streptomycin in a CO₂ incubator at 5% CO₂ and 37 °C.

The cells were plated in 96-well cell culture plates, and different concentrations of NCTD (0-80 µg/mL) were added to the complete cell culture medium. Then, 10 concentrations of NCTD-IRMOF-3 and NCTD-IRMOF-3-Gel were prepared (0-80 µg/mL). After 24, 48, 72, and 96 h of incubation, chemosensitivity was evaluated using thiazolyl blue tetrazolium bromide (MTT reagent, 98%; Wuhan Baodu DE Co., Ltd., Wuhan, China) in complete cell culture medium (5 µg/mL). Then, 20 µL MTT reagent was added to each well and incubated for 4 h, and the mitochondrial aldehyde dehydrogenase from the viable cells subsequently reduced the yellow, water-soluble MTT reagent to water-insoluble blue formazan crystals, which were dissolved by adding 150 µL dimethyl sulfoxide to each well. The absorbance of the dissolved formazan blue dye was measured at 490 nm using a BioTex microplate reader (American Power Instruments Co., Ltd., Wilmington, MA, United States), and the cell viability calculations were performed.

Flow cytometry assay of the effects on the Hepa1-6 cell cycle: The cells were placed in 6-well cell plates and cultured for 24 h in a CO₂ incubator at 5% CO₂ and 37 °C. Then, NCTD-IRMOF-3-Gel at different concentrations (10-40 µg/mL) was added to each well and incubated in an incubator for 24 h. The cells were digested with trypsin (Shanghai Beyotime Biotechnology Co., Ltd., Shanghai, China) and centrifuged at 1500 rpm for 5 min. The supernatant was removed from the solution and washed twice with phosphate-buffered saline (PBS). Then the precooled 75% ethanol solution was added to each well and fixed at 4 °C for 12 h. The solution was centrifuged at 1500 rpm for 5 min to remove the supernatant and resuspended in PBS. Finally, the prepared solution (including 0.5 mL of PBS, 25 µL propidium iodide staining solution and 10 µL ribozyme A) was added to each well and incubated at 37 °C for 30 min. The cells were filtered using a 35 µm cell filter and detected by flow cytometry (Becton, Dickinson and Company, Franklin Lakes, NJ, United States).

Apoptosis experiment: Apoptosis was detected by Annexin V-FITC/PI double staining. K562 cells in the logarithmic growth phase were inoculated into 24-well culture plates at 1×10^5 /well. NCTD-IRMOF-3-Gel, NCTD-IRMOF-3 and NCTD were added at two different concentrations (25 µg/mL and 50 µg/mL). After 48 h, the cells were washed with PBS three times, and 1 µL propidium iodide and 5 µL Annexin V-FITC (Shanghai Beyotime Biotechnology Co., Ltd., Shanghai, China) were added. The cells were incubated in the dark for 10 min and washed once with PBS. Then, 400 µL PBS was added to each tube. Apoptosis was detected by flow cytometry, and the apoptosis rate was calculated.

Statistical analyses

Statistical analyses were performed using analysis of variance with SPSS 24.0 software (version 24.0.0; Chicago, IL, United States). Statistical differences were defined as ^a*P* < 0.05 and ^b*P* < 0.01. The data are presented as the mean ± SD.

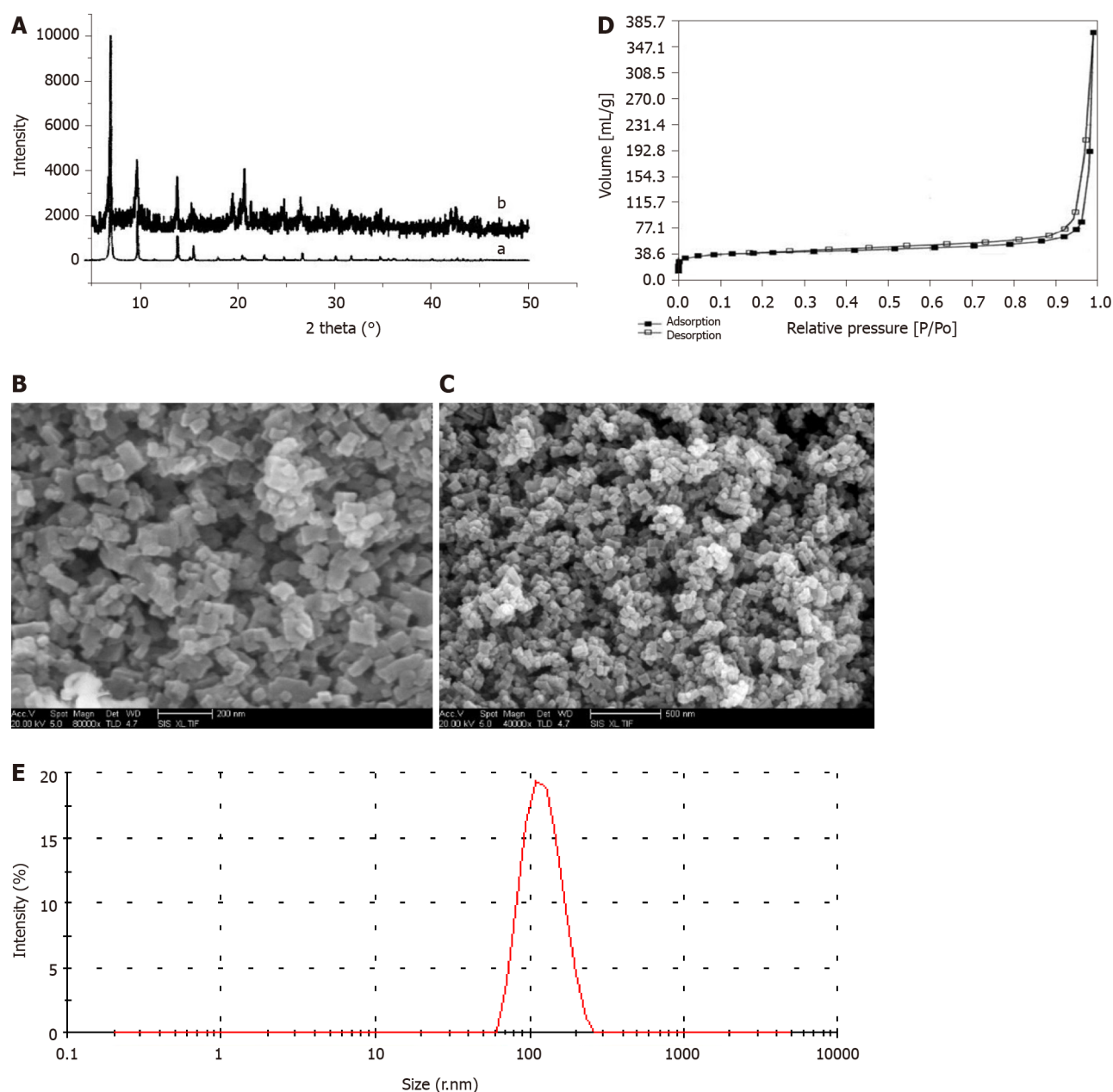


Figure 1 Structure and morphology of IRMOF-3 and norcantharidin-loaded metal-organic framework IRMOF-3 coated with temperature-sensitive gel. A: X-ray diffraction (XRD) spectra of IRMOF-3. Note: XRD patterns of synthetic IRMOF-3 (b) and standard IRMOF-3 (a). XRD patterns of the sample show the same peaks as those of the standard, confirming the high purity of IRMOF-3. The peak patterns of the sample account for the rough appearance of the nanosized particles; B: Scanning electron microscopy (SEM) images of the morphology of IRMOF-3. The particles show a regular square, uniform distribution and a size of 50-100 nm. The single-particle surface is rough, indicating the existence of pores; C: SEM images of the morphology of norcantharidin (NCTD)-loaded metal-organic framework IRMOF-3 coated with temperature-sensitive gel (NCTD-IRMOF-3-Gel). SEM images of the morphology of NCTD-IRMOF-3-Gel showing the same size as that of IRMOF-3; D: Nitrogen adsorption-desorption isotherms of IRMOF-3. Nitrogen adsorption-desorption isotherms. A hysteresis loop phenomenon appears under relatively high pressure, indicating the existence of channels in the sample; E: Particle size distribution of NCTD-IRMOF-3-Gel. The particle size distribution of NCTD-IRMOF-3-Gel indicated that the average particle size was 100 nm.

RESULTS

Structure and morphology

The PXRD patterns shown in Figure 1A illustrate that the IRMOF-3 materials possessed three well-resolved peaks, similar to the standard patterns. The SEM images of IRMOF-3 and NCTD-IRMOF-3-Gel are presented in Figure 1B and Figure 1C which show that the sample consisted of square particles (50-100 nm). The single-particle surface was rough, indicating the existence of pores. SEM images show that the morphology of NCTD-IRMOF-3-Gel had similar size features as those of IRMOF-3. The nitrogen gas (N₂) adsorption-desorption isotherms of IRMOF-3 are shown in Figure 1D. The hysteresis loop phenomenon appeared in the range of relatively high

pressure, indicating the existence of channels in the sample (Figure 1D). The particle size distribution of NCTD-IRMOF-3-Gel indicated that the average particle size was 100 nm (Figure 1E).

NCTD release assay

In the simulated pH 5.0 environment of tumor cells, the drug release data were fitted by a zero-order dynamics equation, first-order kinetic equation, Higuchi equation and Weibull model. The NCTD regression equation obtained is shown in Table 1. The resulting correlation coefficients of the drug release kinetics show that the drug release conforms to the Weibull equation, and the R^2 value is 0.9508.

As shown in Figure 2, the release of NCTD is very fast and is completely finished at 5 h. However, the drug release of NCTD-IRMOF-3 was slower than that of NCTD. The first half of the drug release curve of NCTD was steep and showed a sudden release within 0.6 h. The reason was that the free drug molecules adsorbed on the surface of the nanoparticles diffused rapidly into the medium. Then the curve of NCTD-IRMOF-3 showed a steady slowly release process because the drug in the pores was slowly released. Approximately 5 h were necessary for 50% NCTD release from NCTD-IRMOF-3. After 36 h, the release rate was more than 70%, and the release was basically complete. The release rate of NCTD-IRMOF-3-Gel nanoparticles at 0.3 h was lower than that of the other formulations because NCTD was released gradually with the slow dissolution of poloxamer. After 10 h, the release rate was approximately 50%; after 36 h, the release rate was more than 65%.

In vitro examination

MTT assay: In contrast to that of NCTD- and NCTD-IRMOF-3-treated cells, the inhibition of Hepa1-6 cells treated with NCTD-IRMOF-3-Gel increased in a dose-dependent manner (Figure 3). When the half-maximal inhibitory concentration (IC_{50}) values of each group at different time periods were compared, it was found that these values were 30.59 $\mu\text{g/mL}$, 93.74 $\mu\text{g/mL}$, and 112.3 $\mu\text{g/mL}$ with NCTD, NCTD-IRMOF-3, and NCTD-IRMOF-3-Gel, respectively. The inhibitory effects of NCTD-IRMOF-3-Gel on Hepa1-6 cells were stronger than those of NCTD and NCTD-IRMOF-3 and showed a certain sustained-release effect.

Flow cytometry assay of the effects on the Hepa1-6 cell cycle: Figure 4 and Table 2 show that the percentage of the total number of cells in S phase and G2/M phase increased significantly with increasing NCTD-IRMOF-3-Gel concentration, while the proportion of cells in G0/G1 phase decreased significantly. This result indicates that NCTD-IRMOF-3-Gel can block the cell cycle in the S and G2/M phases, and thermosensitive gel nanoparticles may inhibit cell proliferation by inducing cell cycle arrest.

Apoptosis experiment

It can be seen from the figure that the apoptosis rates of NCTD-IRMOF-3-Gel at the high concentration (C) and low concentration (F) were 32.11 $\mu\text{g/mL}$ and 65.60 $\mu\text{g/mL}$, respectively. Compared with that in the NCTD control group, the apoptosis rate in the NCTD-IRMOF-3-Gel group was highest, which indicated that NCTD-IRMOF-3-Gel could induce the apoptosis of Hepa1-6 cells (Figures 5 and 6).

DISCUSSION

In recent years, with the wide application of medical polymer materials and increased clinical utilization[27,28], research on sustained-release and controlled-release preparations has increased and has become an important research direction. As a new type of drug formulation, sustained- and controlled-release preparations can increase efficacies and reduce side effects compared with traditional drugs. The thermosensitive gel has a hydrophilic three-dimensional network structure, which can be loaded in the liquid state to control drug release. In addition, thermosensitive gel has a stronger affinity, longer retention time and less stimulation in medically relevant locations than traditional gel, especially in mucosal tissue. This type of gel is suitable for all kinds of drug carriers and has now become a research hotspot in pharmaceuticals [29,30].

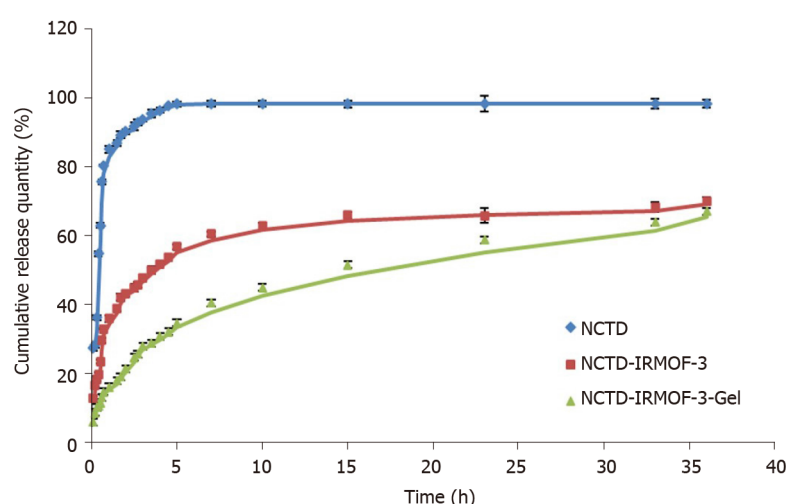
The aim of this project was to prepare NCTD-IRMOF-3-Gel by using the porous material metal-organic framework IRMOF-3 as a drug carrier and NCTD as a model drug. Loading the drug and drug carrier within the thermosensitive gel not only delayed the action time of the drug but also compensated for sudden drug release

Table 1 Release equations and correlation coefficients of norcantharidin-loaded metal-organic framework IRMOF-3 coated with temperature-sensitive gel

	Model	Equation	R^2
DM	Zero-order processes	$Q = 1.2786 t + 36.322$	0.5383
	First-order processes	$\ln(100-Q) = -0.0268 t + 4.1375$	0.667
	Higuchi	$Q = 9.6078 t^{0.5} + 25.29$	0.7719
	Weibull	$\ln \ln(1/(1-Q)) = 0.3813 \ln t - 0.9163$	0.9508

Table 2 Effects of norcantharidin-loaded metal-organic framework IRMOF-3 coated with temperature-sensitive gel on the cell cycle ($n = 3$)

Groups ($\mu\text{g/mL}$)	G0/G1	S	G2/M
Blank group	88.1 ± 2.8	7.2 ± 1.9	4.7 ± 2.1
10	21.9 ± 1.6^b	59.4 ± 2.2^b	18.7 ± 1.8^a
20	16.6 ± 1.2^b	54.1 ± 2.4^b	29.2 ± 1.9^a
40	18.3 ± 2.4^b	45.8 ± 3.1^b	35.8 ± 2.7^a

^a $P < 0.05$.^b $P < 0.01$.**Figure 2** *In vitro* release curves of norcantharidin (NCTD) (blue line), NCTD-loaded metal-organic framework IRMOF-3 (red line), and NCTD-loaded metal-organic framework IRMOF-3 coated with temperature-sensitive gel (green line). After approximately 5 h, 90% of norcantharidin (NCTD) was found in the release medium, while only 50% of NCTD was released from NCTD-loaded metal-organic framework IRMOF-3 (NCTD-IRMOF-3), and 30% of NCTD was released from NCTD-loaded metal-organic framework IRMOF-3 coated with temperature-sensitive gel (NCTD-IRMOF-3-Gel). Every trial was repeated three times. All values are shown as the mean \pm SD.

from the metal-organic framework carrier. The XRD pattern of the IRMOFs is consistent with that of the standard materials and the peak pattern is rough, which suggest that IRMOFs are nanoparticles with rough surfaces and high purity. The SEM images of the morphology of IRMOF-3 and NCTD-IRMOF-3-Gel showed that the IRMOFs were square and regular nanoparticles containing pores. NCTD-IRMOF-3-Gel was prepared using a poloxamer thermosensitive gel as the carrier, and its morphology did not change. This result shows that the thermosensitive gel has no effect on the original metal-organic framework structure, solves the problem of sudden drug release, and can reduce the toxicity caused by sudden drug release.

The Brunauer-Emmett-Teller surface areas and micropore volume of NCTD-IRMOF-3-Gel were determined using N_2 adsorption isotherms, which showed that it was a microporous material. The N_2 adsorption method is commonly used to

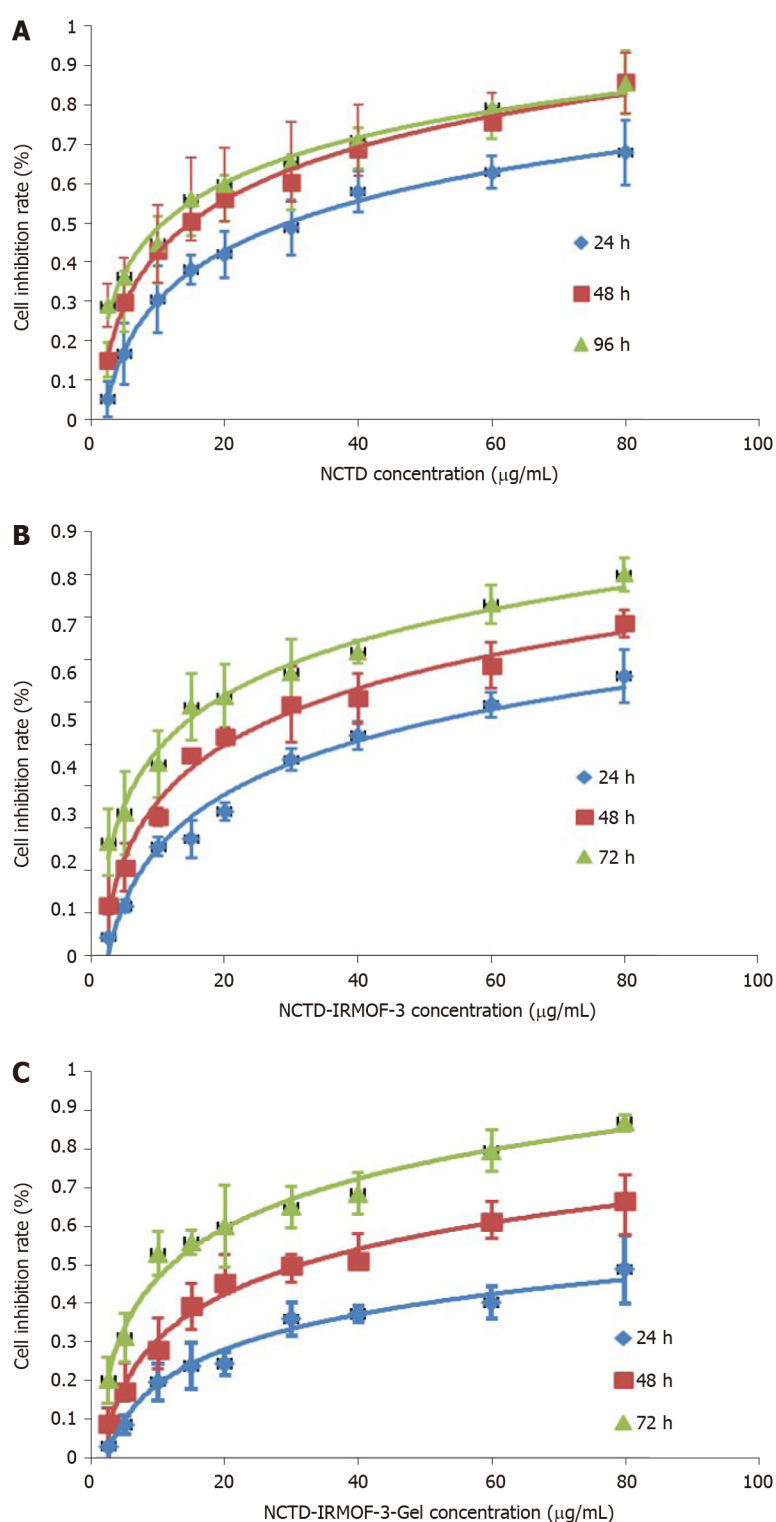


Figure 3 Comparison of the cytotoxicities of norcantharidin (NCTD), NCTD-loaded metal-organic framework IRMOF-3, and NCTD-loaded metal-organic framework IRMOF-3 coated with temperature-sensitive gel. The inhibitory effect of norcantharidin (NCTD)-loaded metal-organic framework IRMOF-3 coated with temperature-sensitive gel (NCTD-IRMOF-3-Gel) (C) on Hepa1-6 cells was stronger than that of NCTD (A) and NCTD-loaded metal-organic framework IRMOF-3 (NCTD-IRMOF-3) (B) and showed a certain sustained-release effect.

determine the specific surface area and pore size of nanomaterials. The determination principle of N_2 adsorption is that the surface pores of porous materials will adsorb nitrogen at liquid nitrogen temperatures. The flat areas in the low-pressure section were caused by the nanopores. The N_2 adsorption quantity increased suddenly, which generated a hysteresis loop, indicating the existence of micropores, and this phenomenon was caused by capillary condensation. After zeta potential analysis of the particle size distribution, NCTD-IRMOF-3-Gel was shown to have a particle size of approximately 100 nm and good dispersibility.

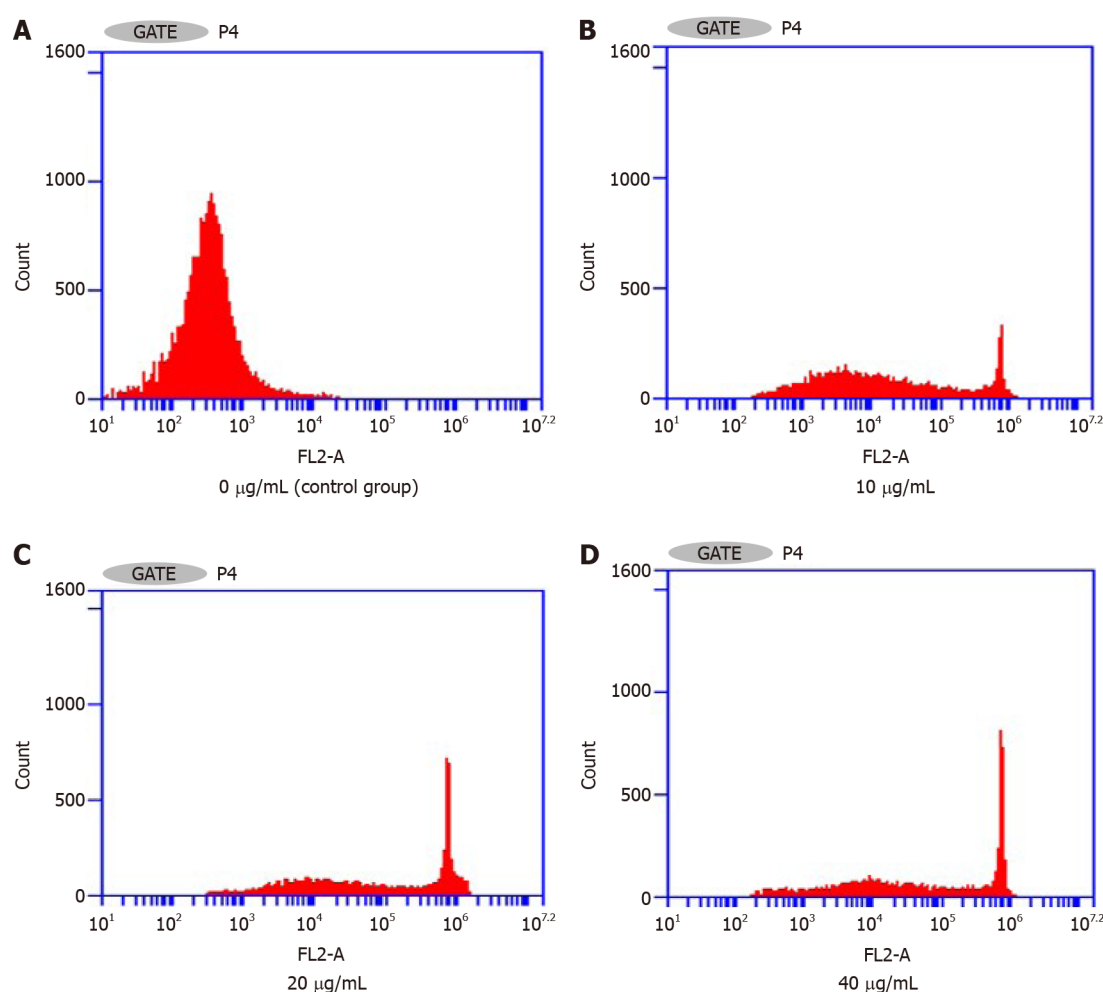


Figure 4 Effects of norcantharidin-loaded metal-organic framework IRMOF-3 coated with temperature-sensitive gel on the cell cycle. The percentage of total cells in S and G2/M phases increased significantly with increasing norcantharidin (NCTD)-loaded metal-organic framework IRMOF-3 coated with temperature-sensitive gel (NCTD-IRMOF-3-Gel) concentration, and the proportion of cells in G0/G1 phase decreased significantly. A: Control group; B: 10 µg/mL; C: 20 µg/mL; D: 40 µg/mL. G1 phase: DNA presynthetic phase, where mitosis is complete before DNA replication begins; G2 phase: DNA synthesis replication phase, where DNA replication is complete before mitosis begins; M phase: Cell division phase; S phase: DNA synthesis replication phase.

The kinetics of *in vitro* drug release can effectively determine the profile of *in vitro* drug release and predict the conditions of *in vivo* drug release. From the drug release curve, NCTD was released quickly, with basically complete release at 5 h. NCTD-IRMOF-3 nanoparticles released NCTD more slowly than free NCTD treatment and showed sudden release within 0.6 h. After 36 h, the release rate was more than 70%, and the release was basically completed. NCTD-IRMOF-3-Gel nanoparticles showed a significantly slower release trend, and the degree of release at 0.3 h was lower than that in the other groups, which was due to the gradual release of NCTD with the slow dissolution of poloxamer. After 36 h, the release rate reached more than 65%. We speculated that NCTD-IRMOF-3-Gel nanoparticles had a certain sustained-release effect and could effectively improve the drug release process.

The MTT assay demonstrated the cytotoxicity of the NCTD-IRMOF-3-Gel nanoparticles. At the same concentration, the inhibition rate of each group of drugs acting on Hepa1-6 cells increased with the extension of time. The inhibition rate of the free drug group was slightly lower than that of the nanoparticle group, but it still had a killing effect on the cells. Compared with that of NCTD-IRMOF-3-Gel, the inhibition rate of NCTD-IRMOF-3 was slightly low, indicating that the thermosensitive gel-coated nanoparticles had a better inhibitory effect on cells. The inhibition rate of the nanoparticle group was low at 24 h and gradually increased after 48 h to the level of inhibition of the free drug, indicating that the drug-loaded nanoparticle-thermosensitive gel group presented an obvious sustained-release effect. Meanwhile, the cell cycle study using flow cytometry showed that NCTD-IRMOF-3-Gel could block the S phase and G2/M phase of the cell cycle, and thermosensitive gel-suspended nanoparticles may inhibit cell proliferation by blocking the cell cycle. The apoptosis

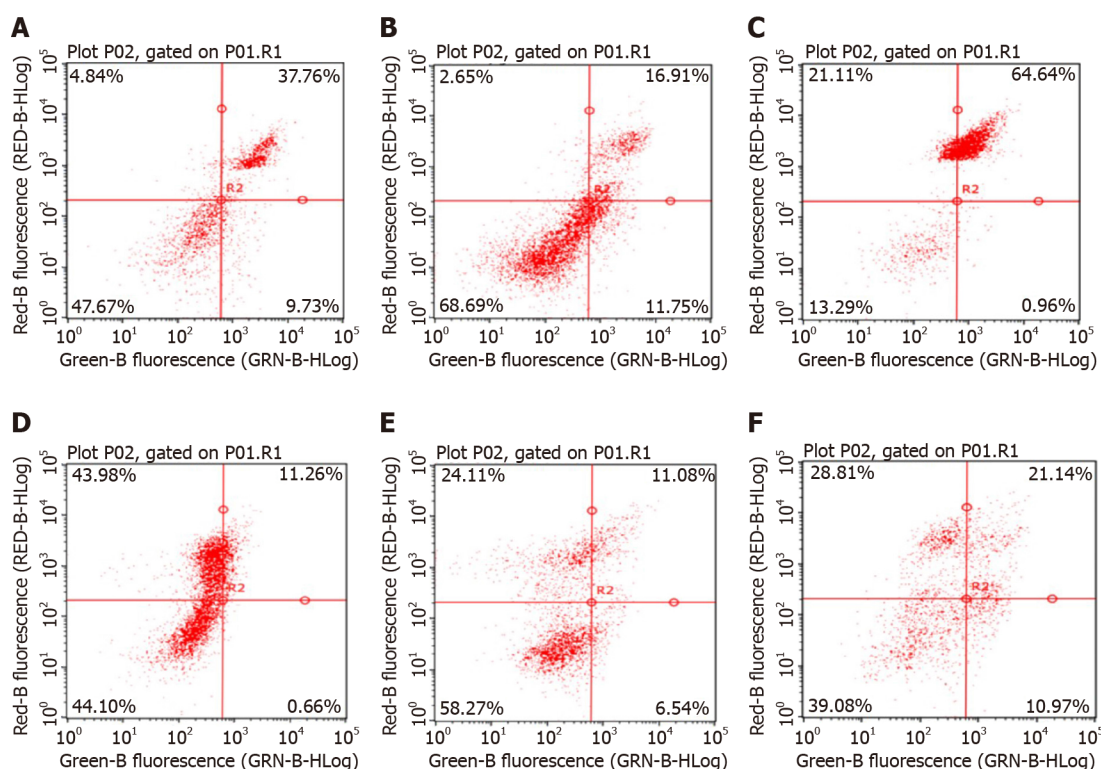


Figure 5 Apoptosis rates of Hepa1-6 cells after 48 h. Apoptosis rates of norcantharidin (NCTD)-loaded metal-organic framework IRMOF-3 coated with temperature-sensitive gel (NCTD-IRMOF-3-Gel) at the high concentration (C) and low concentration (F) were 32.11 $\mu\text{g/mL}$ and 65.60 $\mu\text{g/mL}$, respectively. Compared with the NCTD control group, the apoptosis rate in the NCTD-IRMOF-3-Gel group was highest, which indicated that NCTD-IRMOF-3-Gel could induce the apoptosis of Hepa1-6 cells. A: 50 $\mu\text{g/mL}$ NCTD-IRMOF-3; B: 50 $\mu\text{g/mL}$ NCTD; C: 50 $\mu\text{g/mL}$ NCTD-IRMOF-3-Gel; D: 25 $\mu\text{g/mL}$ NCTD-IRMOF-3; E: 25 $\mu\text{g/mL}$ NCTD; F: 25 $\mu\text{g/mL}$ NCTD-IRMOF-3-Gel.

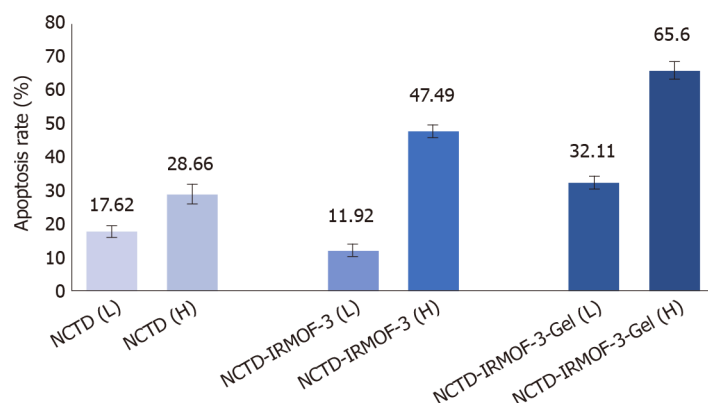


Figure 6 Apoptosis rates of norcantharidin (NCTD), NCTD-loaded metal-organic framework IRMOF-3, and NCTD-loaded metal-organic framework IRMOF-3 coated with temperature-sensitive gel. Compared with the norcantharidin (NCTD) control group, the apoptosis rate in the NCTD-loaded metal-organic framework IRMOF-3 coated with temperature-sensitive gel (NCTD-IRMOF-3-Gel) group was highest, which indicated that NCTD-IRMOF-3-Gel can induce the apoptosis of Hepa1-6 cells.

rates of NCTD-IRMOF-3-Gel at high concentrations and low concentrations were determined, which indicated that NCTD-IRMOF-3-Gel could induce the apoptosis of Hepa1-6 cells.

CONCLUSION

Based on the results of this study, NCTD-loaded IRMOF-3 nanoparticles incorporated into a thermosensitive gel appeared to be a useful tool for cancer treatment because of the enhanced inhibition rate of cancer cells and controlled release of drugs from these

nanocarriers. Our future studies will focus on elucidating the activity of the drug delivery system and its effects on the mechanism of action of the encapsulated anticancer drug.

ARTICLE HIGHLIGHTS

Research background

Norcantharidin (NCTD) is suitable for the treatment of primary liver cancer, especially early and middle primary liver cancer. As a new type of drug formulation, sustained- and controlled-release preparations can increase the efficacy and reduce the side effects compared with traditional drugs. Metal-organic frameworks (MOFs) have potential applications in drug carriers. The thermosensitive gel has a hydrophilic three-dimensional network structure, which can be loaded in the liquid state to control drug release.

Research motivation

The side effects of NCTD have limited its application in liver cancer, which has prompted the development of sustained- and controlled-release preparations.

Research objectives

This study established a liver-targeting therapy in which NCTD is loaded into IRMOF-3 coated with a thermosensitive gel (NCTD-IRMOF-3-Gel), which can be efficiently delivered to liver cancer cells and slowly released.

Research methods

NCTD-loaded IRMOF-3 coated with a temperature-sensitive gel (NCTD-IRMOF-3-Gel) was obtained by a coordination reaction. The apparent characteristics and *in vitro* release of NCTD-IRMOF-3-Gel were investigated. Cell cytotoxicity assays, flow cytometry and apoptosis experiments on mouse hepatoma (Hepa1-6.) cells were used to determine the anti-liver cancer activity of NCTD-IRMOF-3-Gel in *in vitro* models.

Research results

The particle size of NCTD-IRMOF-3-Gel was 50-100 nm, and the particle size distribution was uniform. The release curve showed that NCTD-IRMOF-3-Gel had an obvious sustained-release effect. The cytotoxicity assays showed that the free drug NCTD and NCTD-IRMOF-3-Gel treatments markedly inhibited Hepa1-6 cell proliferation, and with increasing drug concentrations, the inhibition rate increased. By flow cytometry, NCTD-IRMOF-3-Gel was observed to block the Hepa1-6 cell cycle in the S and G2/M phases, and the thermosensitive gel nanoparticles may inhibit cell proliferation by inducing cell cycle arrest. Apoptosis experiments showed that NCTD-IRMOF-3-Gel induced the apoptosis of Hepa1-6 cells.

Research conclusions

NCTD-loaded IRMOF-3 nanoparticles incorporated into a thermosensitive gel appeared to be a useful tool for cancer treatment because of the enhanced inhibition rate of cancer cells and controlled release of drugs from these nanocarriers.

Research perspectives

Thermosensitive gel-encapsulated IRMOF-3 has great advantages as an antitumor drug carrier and provides some ideas for passive targeting therapy of tumors.

ACKNOWLEDGEMENTS

The authors would like to acknowledge Zhang X, Dong S and Xie GL for skillful technical assistance.

REFERENCES

- 1 Forner A, Reig M, Bruix J. Hepatocellular carcinoma. *Lancet* 2018; **391**: 1301-1314 [PMID:

- 29307467 DOI: [10.1016/S0140-6736\(18\)30010-2](https://doi.org/10.1016/S0140-6736(18)30010-2)]
- 2 **Gao Q**, Zhu H, Dong L, Shi W, Chen R, Song Z, Huang C, Li J, Dong X, Zhou Y, Liu Q, Ma L, Wang X, Zhou J, Liu Y, Boja E, Robles AI, Ma W, Wang P, Li Y, Ding L, Wen B, Zhang B, Rodriguez H, Gao D, Zhou H, Fan J. Integrated Proteogenomic Characterization of HBV-Related Hepatocellular Carcinoma. *Cell* 2019; **179**: 561-577. e22 [PMID: [31585088](https://pubmed.ncbi.nlm.nih.gov/31585088/) DOI: [10.1016/j.cell.2019.08.052](https://doi.org/10.1016/j.cell.2019.08.052)]
 - 3 **Orcutt ST**, Anaya DA. Liver Resection and Surgical Strategies for Management of Primary Liver Cancer. *Cancer Control* 2018; **25**: 1073274817744621 [PMID: [29327594](https://pubmed.ncbi.nlm.nih.gov/29327594/) DOI: [10.1177/1073274817744621](https://doi.org/10.1177/1073274817744621)]
 - 4 **Zachos I**, Zachou K, Dalekos GN, Tzortzis V. Management of Patients with Liver Cirrhosis and Invasive Bladder Cancer: A Case-series. *J Transl Int Med* 2019; **7**: 29-33 [PMID: [30997354](https://pubmed.ncbi.nlm.nih.gov/30997354/) DOI: [10.2478/jtim-2019-0006](https://doi.org/10.2478/jtim-2019-0006)]
 - 5 **Power DG**, Kemeny NE. Chemotherapy for the conversion of unresectable colorectal cancer liver metastases to resection. *Crit Rev Oncol Hematol* 2011; **79**: 251-264 [PMID: [20970353](https://pubmed.ncbi.nlm.nih.gov/20970353/) DOI: [10.1016/j.critrevonc.2010.08.001](https://doi.org/10.1016/j.critrevonc.2010.08.001)]
 - 6 **Mohri J**, Katada C, Ueda M, Sugawara M, Yamashita K, Moriya H, Komori S, Hayakawa K, Koizumi W, Atsuda K. Predisposing Factors for Chemotherapy-induced Nephrotoxicity in Patients with Advanced Esophageal Cancer Who Received Combination Chemotherapy with Docetaxel, Cisplatin, and 5-fluorouracil. *J Transl Int Med* 2018; **6**: 32-37 [PMID: [29607302](https://pubmed.ncbi.nlm.nih.gov/29607302/) DOI: [10.2478/jtim-2018-0007](https://doi.org/10.2478/jtim-2018-0007)]
 - 7 **Michael JS**, Lee BS, Zhang M, Yu JS. Nanotechnology for Treatment of Glioblastoma Multiforme. *J Transl Int Med* 2018; **6**: 128-133 [PMID: [30425948](https://pubmed.ncbi.nlm.nih.gov/30425948/) DOI: [10.2478/jtim-2018-0025](https://doi.org/10.2478/jtim-2018-0025)]
 - 8 **Andrašina T**, Rohan T, Hustý J, Válek V. Interventional radiology therapies for liver cancer. *Cas Lek Cesk* 2018; **157**: 195-202 [PMID: [30189743](https://pubmed.ncbi.nlm.nih.gov/30189743/)]
 - 9 **Chi J**, Jiang Z, Qiao J, Zhang W, Peng Y, Liu W, Han B. Antitumor evaluation of carboxymethyl chitosan based norcantharidin conjugates against gastric cancer as novel polymer therapeutics. *Int J Biol Macromol* 2019; **136**: 1-12 [PMID: [31158420](https://pubmed.ncbi.nlm.nih.gov/31158420/) DOI: [10.1016/j.ijbiomac.2019.05.216](https://doi.org/10.1016/j.ijbiomac.2019.05.216)]
 - 10 **Lv H**, Li Y, Du H, Fang J, Song X, Zhang J. The Synthetic Compound Norcantharidin Induced Apoptosis in Mantle Cell Lymphoma In Vivo and In Vitro through the PI3K-Akt-NF- κ B Signaling Pathway. *Evid Based Complement Alternat Med* 2013; **2013**: 461487 [PMID: [23935664](https://pubmed.ncbi.nlm.nih.gov/23935664/) DOI: [10.1155/2013/461487](https://doi.org/10.1155/2013/461487)]
 - 11 **Jin D**, Wu Y, Shao C, Gao Y, Wang D, Guo J. Norcantharidin reverses cisplatin resistance and inhibits the epithelial mesenchymal transition of human nonsmall lung cancer cells by regulating the YAP pathway. *Oncol Rep* 2018; **40**: 609-620 [PMID: [29901163](https://pubmed.ncbi.nlm.nih.gov/29901163/) DOI: [10.3892/or.2018.6486](https://doi.org/10.3892/or.2018.6486)]
 - 12 **Zhang Z**, Yang L, Hou J, Xia X, Wang J, Ning Q, Jiang S. Promising positive liver targeting delivery system based on arabinogalactan-anchored polymeric micelles of norcantharidin. *Artif Cells Nanomed Biotechnol* 2018; **46**: S630-S640 [PMID: [30449176](https://pubmed.ncbi.nlm.nih.gov/30449176/) DOI: [10.1080/21691401.2018.1505742](https://doi.org/10.1080/21691401.2018.1505742)]
 - 13 **Zhou J**, Ren Y, Tan L, Song X, Wang M, Li Y, Cao Z, Guo C. Norcantharidin: research advances in pharmaceutical activities and derivatives in recent years. *Biomed Pharmacother* 2020; **131**: 110755 [PMID: [33152920](https://pubmed.ncbi.nlm.nih.gov/33152920/) DOI: [10.1016/j.biopha.2020.110755](https://doi.org/10.1016/j.biopha.2020.110755)]
 - 14 **Deng L**, Tang S. Norcantharidin analogues: a patent review (2006 - 2010). *Expert Opin Ther Pat* 2011; **21**: 1743-1753 [PMID: [22017412](https://pubmed.ncbi.nlm.nih.gov/22017412/) DOI: [10.1517/13543776.2011.629190](https://doi.org/10.1517/13543776.2011.629190)]
 - 15 **Mo L**, Zhang X, Shi X, Wei L, Zheng D, Li H, Gao J, Li J, Hu Z. Norcantharidin enhances antitumor immunity of GM-CSF prostate cancer cells vaccine by inducing apoptosis of regulatory T cells. *Cancer Sci* 2018; **109**: 2109-2118 [PMID: [29770533](https://pubmed.ncbi.nlm.nih.gov/29770533/) DOI: [10.1111/cas.13639](https://doi.org/10.1111/cas.13639)]
 - 16 **Wei CM**, Wang BJ, Ma Y, Sun ZP, Li XL, Guo RC. [Pharmacokinetics and biodistribution of 3H-norcantharidin in mice]. *Yao Xue Xue Bao* 2007; **42**: 516-519 [PMID: [17703775](https://pubmed.ncbi.nlm.nih.gov/17703775/)]
 - 17 **Zhang R**, Wang J, Yuan G, Wei C, Liu X, Wang B, Gao H, Guo R. Determination of norcantharidin in mouse tissues by liquid chromatography coupled to tandem mass spectrometry and its tissue distribution study. *Arzneimittelforschung* 2012; **62**: 290-294 [PMID: [22473525](https://pubmed.ncbi.nlm.nih.gov/22473525/) DOI: [10.1055/s-0032-1308980](https://doi.org/10.1055/s-0032-1308980)]
 - 18 **Chen YC**, Chang SC, Wu MH, Chuang KA, Wu JY, Tsai WJ, Kuo YC. Norcantharidin reduced cyclins and cytokines production in human peripheral blood mononuclear cells. *Life Sci* 2009; **84**: 218-226 [PMID: [19100750](https://pubmed.ncbi.nlm.nih.gov/19100750/) DOI: [10.1016/j.lfs.2008.11.020](https://doi.org/10.1016/j.lfs.2008.11.020)]
 - 19 **Zhang J**, Shen D, Jia M, Zhao H, Tang Y. The targeting effect of Hm²E8b-NCTD-liposomes on B-lineage leukaemia stem cells is associated with the HLF-SLUG axis. *J Drug Target* 2018; **26**: 55-65 [PMID: [28627280](https://pubmed.ncbi.nlm.nih.gov/28627280/) DOI: [10.1080/1061186X.2017.1339193](https://doi.org/10.1080/1061186X.2017.1339193)]
 - 20 **Zeng L**, Zhang Y. Development, optimization and *in vitro* evaluation of norcantharidin loaded self-nanoemulsifying drug delivery systems (NCTD-SNEDDS). *Pharm Dev Technol* 2017; **22**: 399-408 [PMID: [27487261](https://pubmed.ncbi.nlm.nih.gov/27487261/) DOI: [10.1080/10837450.2016.1219915](https://doi.org/10.1080/10837450.2016.1219915)]
 - 21 **Zeng L**, Liu Y, Pan J, Liu X. Formulation and evaluation of norcantharidin nanoemulsions against the *Plutella xylostella* (Lepidoptera: Plutellidae). *BMC Biotechnol* 2019; **19**: 16 [PMID: [30871528](https://pubmed.ncbi.nlm.nih.gov/30871528/) DOI: [10.1186/s12896-019-0508-8](https://doi.org/10.1186/s12896-019-0508-8)]
 - 22 **Zhu J**, Zhang W, Wang D, Li S, Wu W. Preparation and characterization of norcantharidin liposomes modified with stearyl glycyrrhetinate. *Exp Ther Med* 2018; **16**: 1639-1646 [PMID: [30186382](https://pubmed.ncbi.nlm.nih.gov/30186382/) DOI: [10.3892/etm.2018.6416](https://doi.org/10.3892/etm.2018.6416)]
 - 23 **Li Y**, Li X, Guan Q, Zhang C, Xu T, Dong Y, Bai X, Zhang W. Strategy for chemotherapeutic delivery using a nanosized porous metal-organic framework with a central composite design. *Int J Nanomedicine* 2017; **12**: 1465-1474 [PMID: [28260892](https://pubmed.ncbi.nlm.nih.gov/28260892/) DOI: [10.2147/IJN.S119115](https://doi.org/10.2147/IJN.S119115)]

- 24 **Zhao H**, Hou S, Zhao X, Liu D. Adsorption and pH-responsive release of tinidazole on metal-organic framework CAU-1. *Chem Eng Data* 2019; **64**: 1851-1858 [DOI: [10.1021/acs.jced.9b00106](https://doi.org/10.1021/acs.jced.9b00106)]
- 25 **Lin SX**, Pan WL, Niu RJ, Liu Y, Chen JX, Zhang WH, Lang JP, Young DJ. Effective loading of cisplatin into a nanoscale UiO-66 metal-organic framework with preformed defects. *Dalton Trans* 2019; **48**: 5308-5314 [PMID: [30938739](https://pubmed.ncbi.nlm.nih.gov/30938739/) DOI: [10.1039/c9dt00719a](https://doi.org/10.1039/c9dt00719a)]
- 26 **Nezhad-Mokhtari P**, Arsalani N, Javanbakht S, Shaabani A. Development of gelatin microsphere encapsulated Cu-based metal-organic framework nanohybrid for the methotrexate delivery. *J Drug Deliv Sci Technol* 2019; **50**: 174-180 [DOI: [10.1016/j.jddst.2019.01.020](https://doi.org/10.1016/j.jddst.2019.01.020)]
- 27 **Nasrollahi P**, Khajeh K, Tamjid E, Taleb M, Soleimani M, Nie G. Sustained release of sodium deoxycholate from PLGA-PEG-PLGA thermosensitive polymer. *Artif Cells Nanomed Biotechnol* 2018; **46**: 1170-1177 [PMID: [29989444](https://pubmed.ncbi.nlm.nih.gov/29989444/) DOI: [10.1080/21691401.2018.1481861](https://doi.org/10.1080/21691401.2018.1481861)]
- 28 **Abulateefeh SR**, Alkawareek MY, Alkilany AM. Tunable sustained release drug delivery system based on mononuclear aqueous core-polymer shell microcapsules. *Int J Pharm* 2019; **558**: 291-298 [PMID: [30641178](https://pubmed.ncbi.nlm.nih.gov/30641178/) DOI: [10.1016/j.ijpharm.2019.01.006](https://doi.org/10.1016/j.ijpharm.2019.01.006)]
- 29 **Svirskis D**, Chandramouli K, Bhusal P, Wu Z, Alphonso J, Chow J, Patel D, Ramakrishna R, Yeo SJ, Stowers R, Hill A, Munro J, Young SW, Sharma M. Injectable thermosensitive gelling delivery system for the sustained release of lidocaine. *Ther Deliv* 2016; **7**: 359-368 [PMID: [27250538](https://pubmed.ncbi.nlm.nih.gov/27250538/) DOI: [10.4155/tde-2016-0014](https://doi.org/10.4155/tde-2016-0014)]
- 30 **Liu Y**, Wang X, Liu Y, Di X. Thermosensitive In Situ Gel Based on Solid Dispersion for Rectal Delivery of Ibuprofen. *AAPS PharmSciTech* 2018; **19**: 338-347 [PMID: [28733828](https://pubmed.ncbi.nlm.nih.gov/28733828/) DOI: [10.1208/s12249-017-0839-5](https://doi.org/10.1208/s12249-017-0839-5)]



Published by **Baishideng Publishing Group Inc**
7041 Koll Center Parkway, Suite 160, Pleasanton, CA 94566, USA

Telephone: +1-925-3991568

E-mail: bpgoffice@wjgnet.com

Help Desk: <https://www.f6publishing.com/helpdesk>

<https://www.wjgnet.com>

